

Supporting Information

Structure Engineering to Maintain Superior Capacitance of Molybdenum Oxides at Ultrahigh Mass Loadings

Ji-Chi Liu,¹ Hui Li,¹ Munkhbayar Batmunkh,² Xue Xiao,³ Ying Sun,¹ Qin Zhao,¹ Xue Liu,¹ Zi-Hang
Huang,^{1,*} and Tian-Yi Ma^{3,*}

¹Institute of Clean Energy Chemistry, Key Laboratory for Green Synthesis and Preparative
Chemistry of Advanced Materials, College of Chemistry, Liaoning University, Shenyang 110036,
China

²Australian Institute for Bioengineering and Nanotechnology, University of Queensland, St. Lucia,
QLD, 4072 Australia

³Discipline of Chemistry, University of Newcastle, Callaghan, NSW 2308, Australia

* Corresponding authors: Tian-Yi Ma, Tianyi.Ma@newcastle.edu.au
Zi-Hang Huang, huangzihang@lnu.edu.cn

1. Methods

1.1 Materials

Graphite foil (G) was purchased from SGL group company, Germany. The other reagents were purchased from Aladdin Chemicals and used as received.

1.2 Preparation of functionalized partial-exfoliated graphite (FEG) substrate

The FEG substrate was obtained by two electrochemical steps reported in the previous publication.¹ In the first step, the G (1 cm×1 cm) was potential dynamically scanned between 0.5 and 1.8 V at 20 mV s⁻¹ in 0.5 M K₂CO₃ aqueous solution for 8 cycles, with a platinum plate and saturated calomel electrode (SCE) as the counter and reference electrodes, respectively. Subsequently, the working electrode was treated in 0.5 M KNO₃ electrolyte at constant potential of 1.8 V versus SCE for 2.5 h to generate functional groups. To recover the electrical conductivity of the oxidized graphite layers, the electrode was cycled between -1 to 0.9 V versus SCE at 50 mV s⁻¹ in 3 M KCl aqueous solution for 50 cycles. Finally, the FEG substrate was washed with deionized water and ethanol to remove the residual electrolyte. The dimension of FEG substrate is 1 cm×1 cm (length×width).

1.3 Electrochemical deposition of MoO_{3-x}

Molybdenum oxide was carried out by electrodeposition on FEG, using 0.02 M ammonium molybdate aqueous electrolyte with graphite foil counter and SCE reference electrodes. A constant potential of -1.5 V versus SCE was applied for 40 min. The fabricated electrode was washed with deionized water and denoted as FEG/MoO_{3-x}. The loading was around 15.4 mg cm⁻². The deposition was also carried out for periods varying from 10 to 50 min while other conditions were kept constant. For comparison, MoO_{3-x} was also electrodeposited on graphite foil and carbon cloth substrates directly under the same experimental conditions and denoted as G/MoO_{3-x} and CC/MoO_{3-x}.

1.4 Assembly of FEG/MoO_{3-x}//FEG ASC device

A model ASC device was assembled by using FEG/MoO_{3-x} as the negative electrode and FEG as the positive electrode. A piece of cellulose paper (NKK separator, Japan) as a separator were soaked in a 3 M KCl or KCl/PVA electrolyte for 5 min. The entire device was wrapped and sealed with parafilm to prevent electrolyte from drying. The working area of the device was 1.0 cm². The volume of the device (including the volume of two electrodes and separator) was 0.252 cm³ [1 cm (L)×1 cm (W)×0.252 cm (H)].

1.5 Characterizations

The morphology of the electrodes were characterized by a scanning electron microscope (SEM) equipped with an energy dispersive X-ray spectroscopy (EDS) detector (HITACHI, SU8010, Japan). Transmission electron microscope (TEM) images were collected by JEM-2010. X-ray photoelectron spectroscopy (XPS) was measured on an XPS spectrometer (ESCALAB 250Xi, Thermo Scientific Escalab, USA) with Al-K α radiation (8.34 Å) as the excitation source. The data was calibrated by referencing the C 1s peak to 284.6 eV. The crystal structures of the samples were characterized by X-ray diffraction (Bruker D8-Advance). The mass loading of the active materials was measured using a microbalance with a sensitivity of 0.01 mg (BT 25 S, Sartorius, Germany).

1.6 Electrochemical tests

Electrochemical measurements were conducted using a CHI 760E electrochemical work station. The electrochemical performance of FEG/MoO_{3-x} samples was tested in a three-electrode cell with SCE electrode and graphite foil as the reference and counter electrode, respectively, in 3 M KCl electrolyte. Electrochemical performance of the FEG/MoO_{3-x}//FEG was evaluated using a two-electrode testing system. EIS was carried out at open-circuit potentials with a perturbation of 10 mV and in a frequency range from 0.01 Hz to 40 kHz.

2. Calculations

2.1 Capacitances of single electrode

The areal and gravimetric capacitance of a single electrode can be calculated based on galvanostatic charge-discharge experiments according to Equation S1 and S2:

$$C_s = \frac{I \times t}{\Delta U \times S} \quad (\text{Equation S1})$$

$$C_m = \frac{I \times t}{\Delta U \times m} \quad (\text{Equation S2})$$

where C_s and C_m (mF cm⁻² or F g⁻¹) are the areal and gravimetric capacitance, I is the discharge current (mA), t is the time (s), ΔU is the potential window (V), S is the working area of electrode (cm²), m is the mass of active material.

2.2 Capacitances of ASC Devices

The volumetric capacitance (C_V , unit in F cm⁻³) of the FEG/MoO_{3-x}//FEG device can be calculated based on galvanostatic charge-discharge experiments according to Equation S3:

$$C_V = \frac{I \times t}{U \times V} \quad (\text{Equation S3})$$

where I is the charge-discharge current (A), t is the discharge time (s), U is the operating voltage and V is the total volume (cm³) of the whole device stack including two electrodes, electrolyte-soaked separator, as well as the package.

The areal capacitance of ASC device can be calculated based on galvanostatic charge-discharge experiments according to Equation S4:

$$C_s = \frac{I \times t}{U \times S} \quad (\text{Equation S4})$$

where C_S (mF cm⁻²) is the areal capacitance of the ASC, I is the discharge current (mA), t is the time (s), U is the operating voltage of the ASC (V), S is the working area of electrode (cm²).

2.3 Volumetric energy density and power density of FEG/MoO_{3-x}//FEG Devices

Volumetric energy density (E , Wh cm⁻³) and power density (P , W cm⁻³) of the devices are calculated using the following equations:

$$E_V = \frac{C_V \times U^2}{2 \times 3600} \quad (\text{Equation S5})$$

$$P_V = \frac{3600 \times E_V}{t} \quad (\text{Equation S6})$$

Where C_V (F cm⁻³) is the specific capacitance, U is the operating voltage (V) and t is the discharge time (s).

2.4 Charge balance for FEG/MoO_{3-x}//FEG Devices

To achieve the maximum and stable performance of the ASC device, the capacity (Q) of negative and positive electrode should be balanced, *i.e.*,

$$Q_- = Q_+ \quad (\text{Equation S7})$$

The capacity is associated with areal capacitance (C_s), potential window (ΔU) and working area of electrode (S), as shown in Equation S8:

$$Q = C_s \times \Delta U \times S \quad (\text{Equation S8})$$

Combining Equation S7 and S8, the areal capacitance of negative electrode to positive electrode should satisfy Equation S9:

$$\frac{C_{s,-}}{C_{s,+}} = \frac{(S_+) \times (\Delta U_+)}{(S_-) \times (\Delta U_-)} \quad (\text{Equation S9})$$

In our work, we fixed the working area of both electrodes at 1.0 cm². Substitute $\Delta U_- = 0.7$ V and $\Delta U_+ = 1.3$ V. According to Equation S9, the ratio of areal capacitance of FEG/MoO_{3-x} to FEG

electrode is ~ 1.8 , which is close to the areal capacitance of FEG/MoO_{3-x} (4.3 F cm⁻²) to FEG (2.3 F cm⁻²) used in our work.

3. Supplementary Figures and Tables

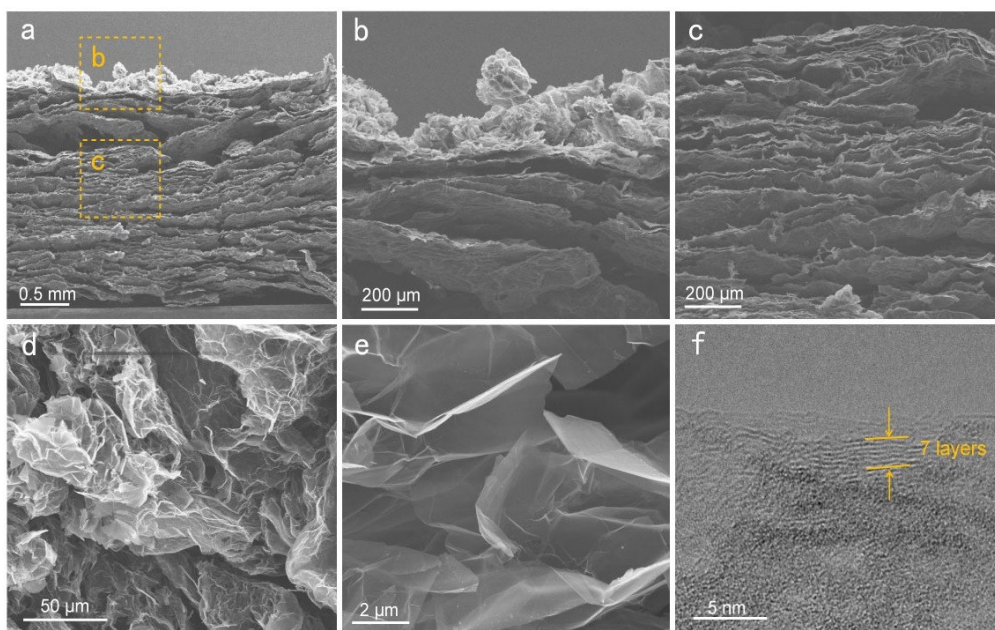


Fig. S1 Side (a-c) and top (d-e) view SEM images of FEG. (f) TEM image of ultrasonicated FEG sample.

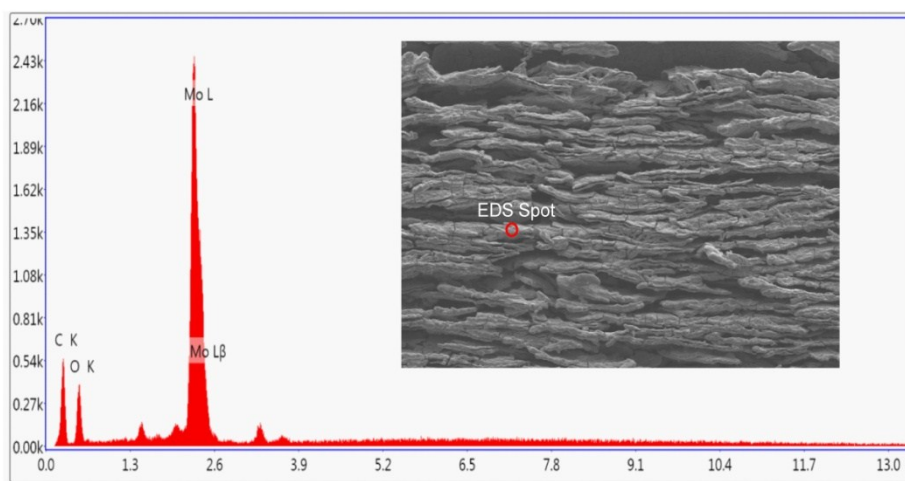


Fig. S2 EDS spectra collected for FEG/MoO_{3-x} sample.

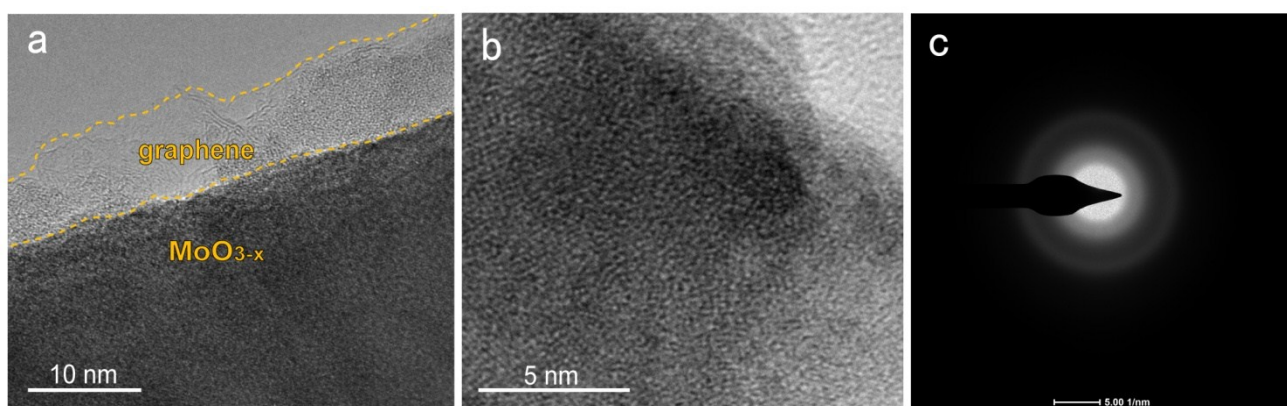


Fig. S3 High-resolution TEM images (a, b) of the FEG/MoO_{3-x} sample and (c) the corresponding SAED pattern.

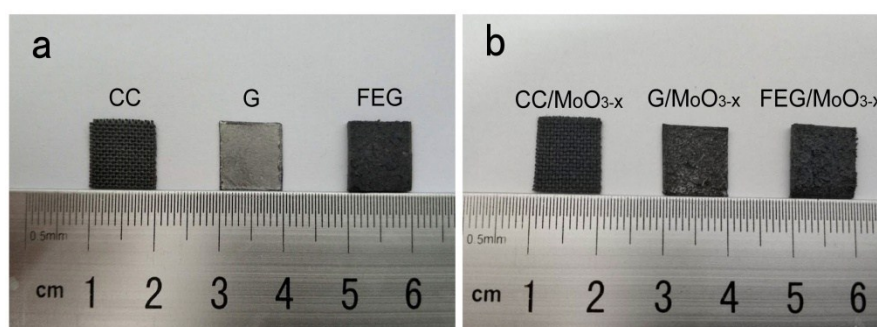


Fig. S4 Digital pictures of as-prepared electrodes: (a) CC, G and FEG electrodes; (b) CC/MoO_{3-x}, G/MoO_{3-x} and FEG/MoO_{3-x} electrodes.

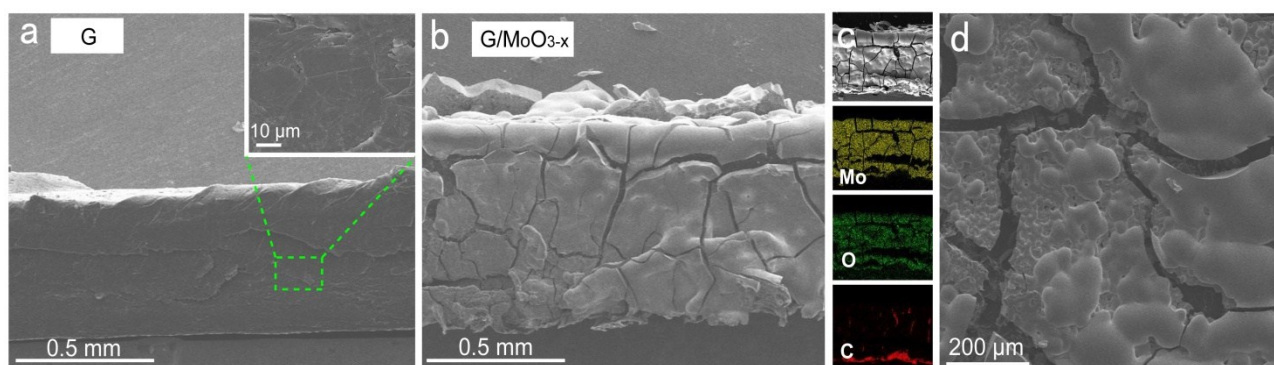


Fig. S5 Side view SEM images of (a) G and (b) G/MoO_{3-x}. (c) Elemental mapping (Mo *K_{α1}*, O *K_{α1}* and C *K_{α1}*) images of G/MoO_{3-x}. (d) Top view SEM image of G/MoO_{3-x} sample.

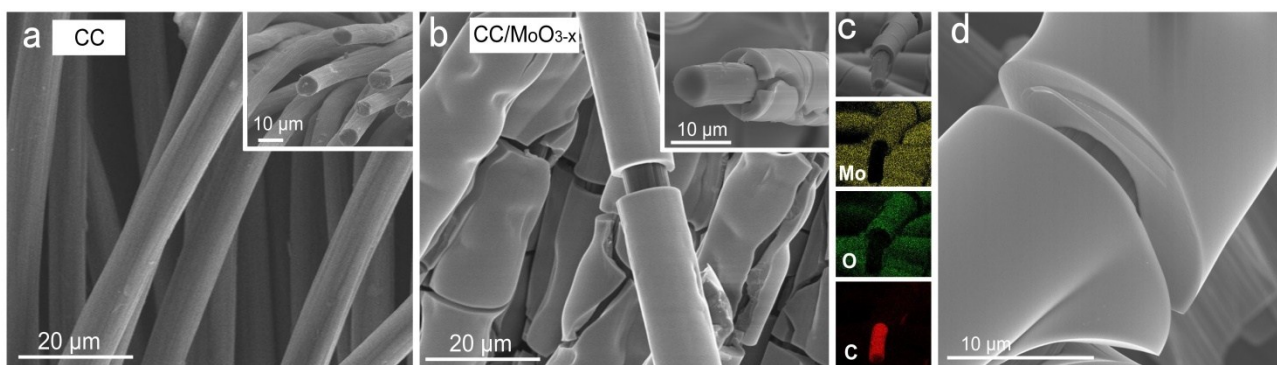


Fig. S6 SEM images of (a) CC and (b) CC/MoO_{3-x}. Insets show the cross sectional images of these samples. (c) Elemental mapping (Mo *K_{α1}*, O *K_{α1}* and C *K_{α1}*) images of CC/MoO_{3-x}. (d) High-magnification SEM image of CC/MoO_{3-x} sample.

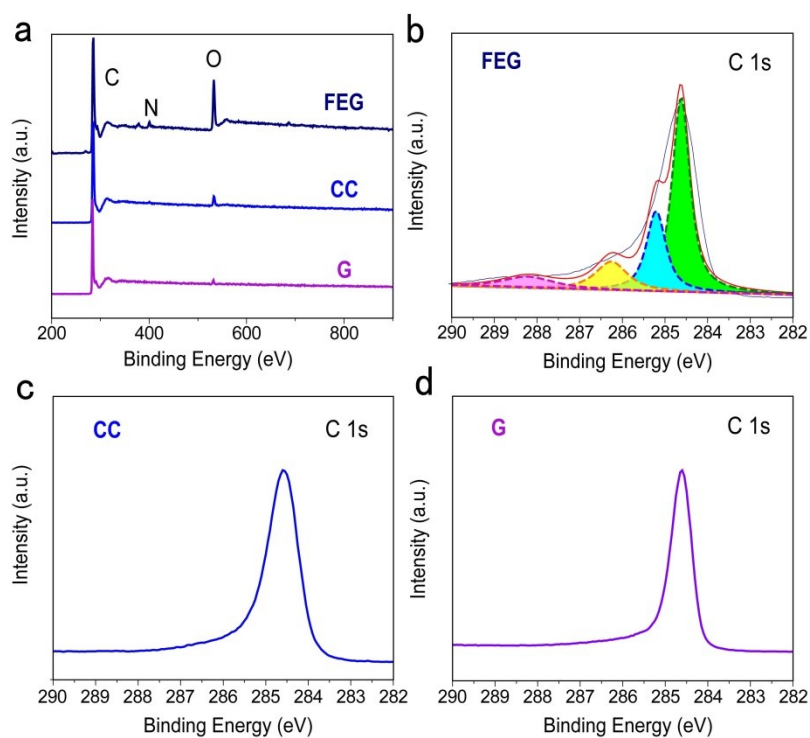


Fig. S7 XPS survey spectrum of FEG, CC, and G electrodes (a). High resolution C 1s XPS peaks of FEG (b), CC (c), and G (d) electrodes.

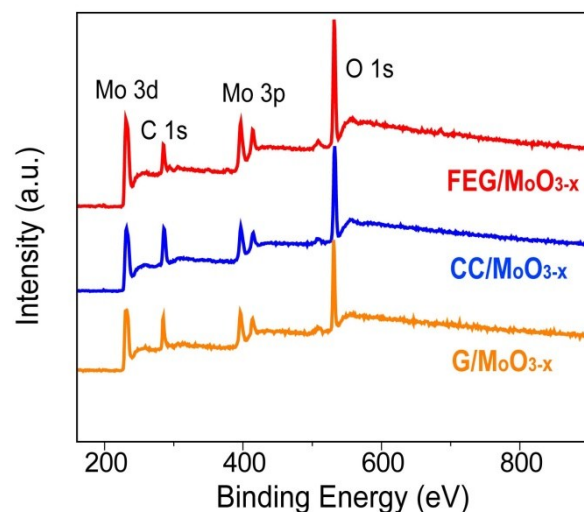


Fig. S8 XPS survey spectrum of FEG/MoO_{3-x}, CC/MoO_{3-x}, and G/MoO_{3-x} electrodes.

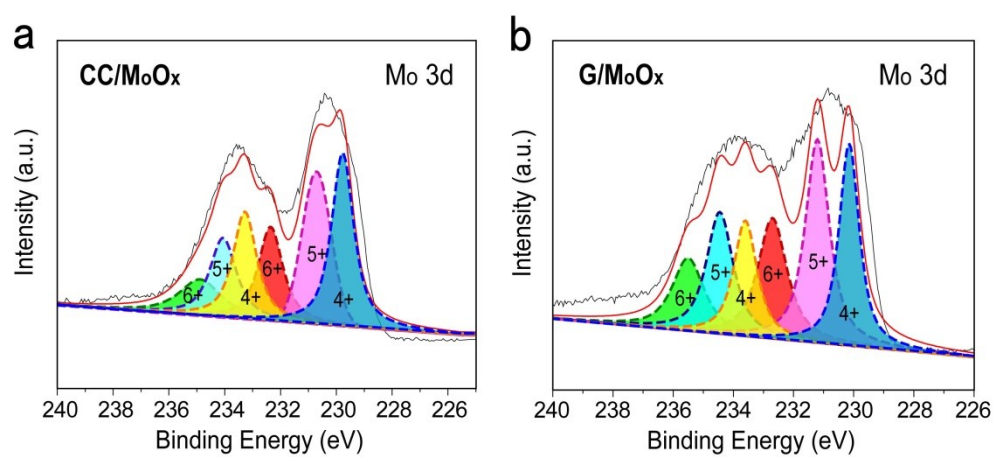


Fig. S9 The Mo 3d XPS peak of G/MoO_{3-x} and CC/MoO_{3-x} electrodes.

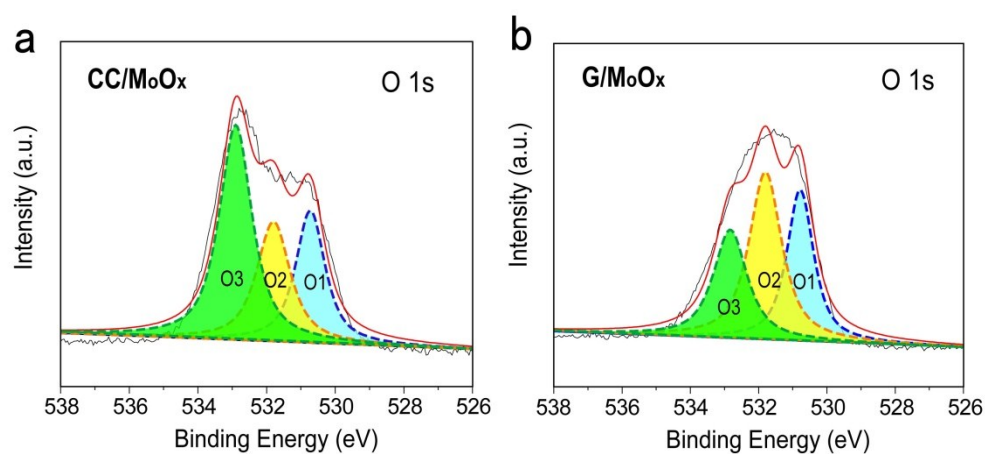


Fig. S10 O 1s XPS peak of G/MoO_{3-x} and CC/MoO_{3-x} electrodes.

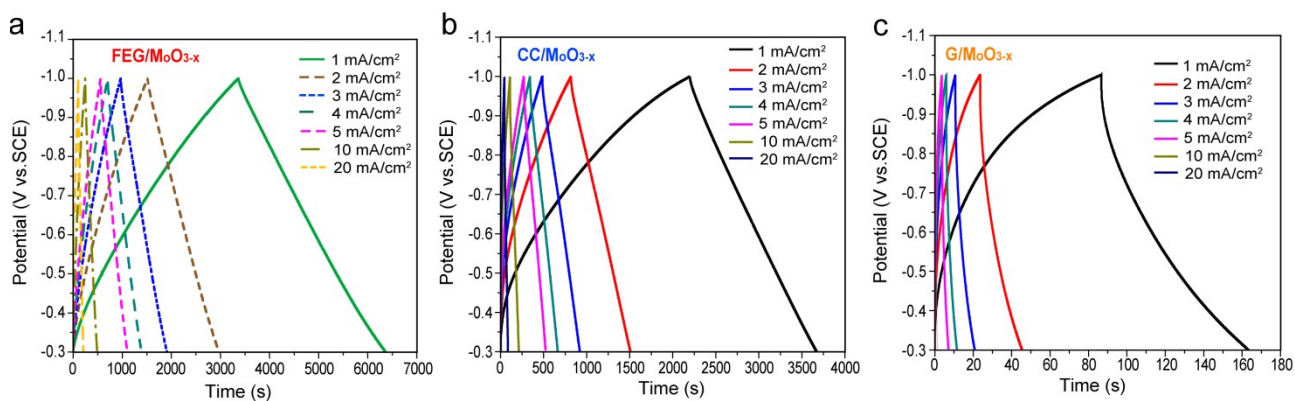


Fig. S11 Galvanostatic charge-discharge (GCD) profiles of FEG/MoO_{3-x} (a), CC/MoO_{3-x} (b) and G/MoO_{3-x} (c) electrodes collected at various current densities.

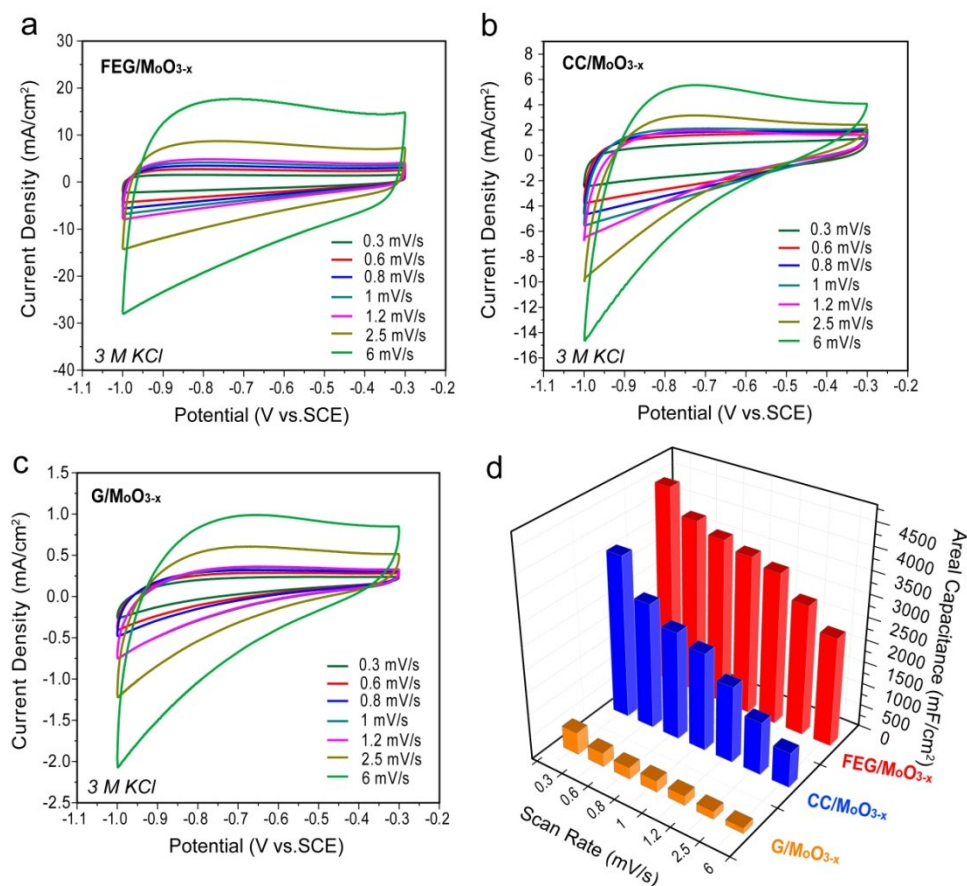


Fig. S12 CV curves of the FEG/MoO_{3-x} (a), CC/MoO_{3-x} (b), and G/MoO_{3-x} (c) electrodes measured at different scan rates. Areal capacitance of the three electrodes (d) measured by CV curves.

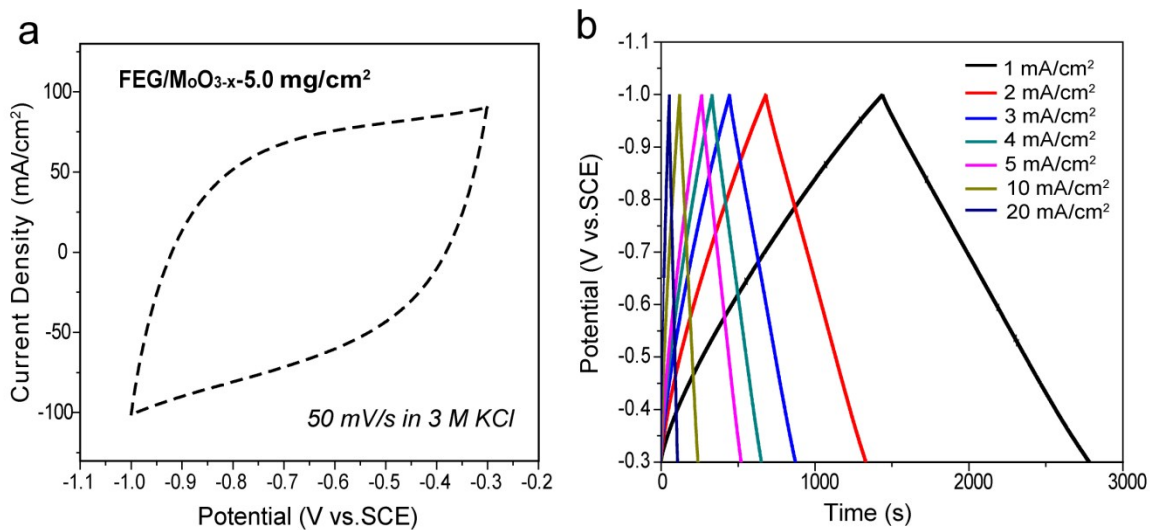


Fig. S13 (a) CV curve of FEG/MoO_{3-x} (5.0 mg cm⁻²) electrode measured at a scan rate of 50 mV s⁻¹.

(b) GCD profiles of FEG/MoO_{3-x} (5.0 mg cm⁻²) collected at various current densities.

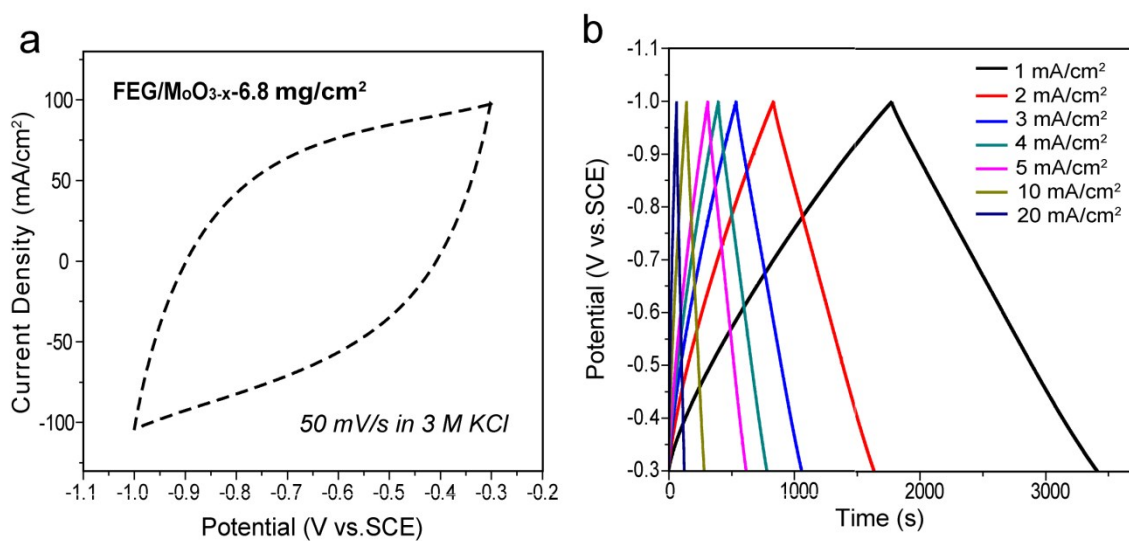


Fig. S14 (a) CV curve of FEG/MoO_{3-x} (6.8 mg cm⁻²) electrode measured at a scan rate of 50 mV s⁻¹.

(b) GCD profiles of FEG/MoO_{3-x} (6.8 mg cm⁻²) collected at various current densities.

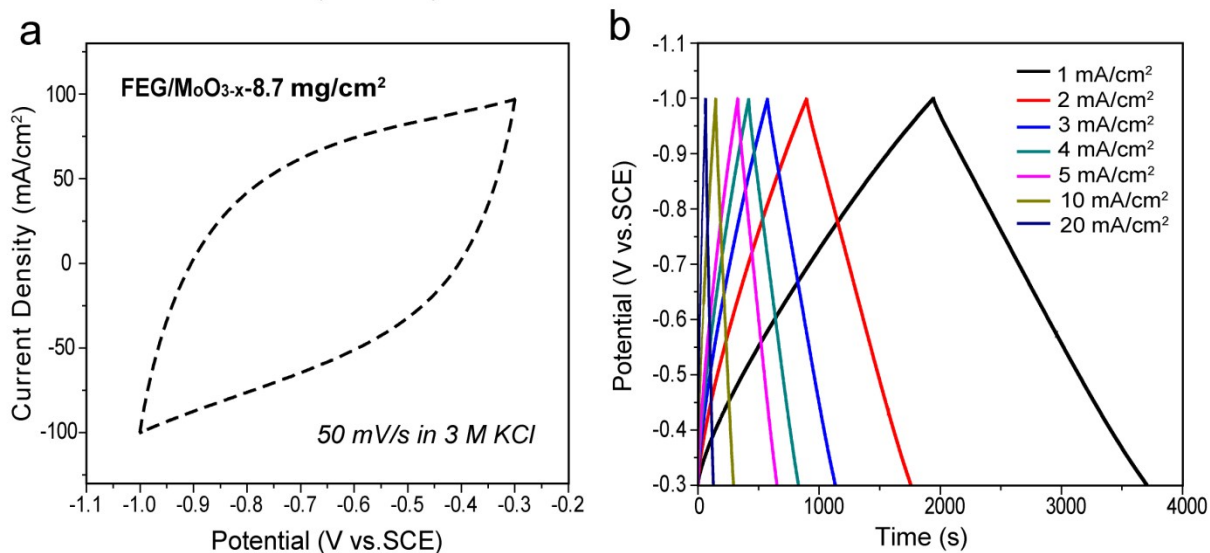


Fig. S15 (a) CV curve of FEG/MoO_{3-x} (8.7 mg cm⁻²) electrode measured at a scan rate of 50 mV s⁻¹.

(b) GCD profiles of FEG/MoO_{3-x} (8.7 mg cm⁻²) collected at various current densities.

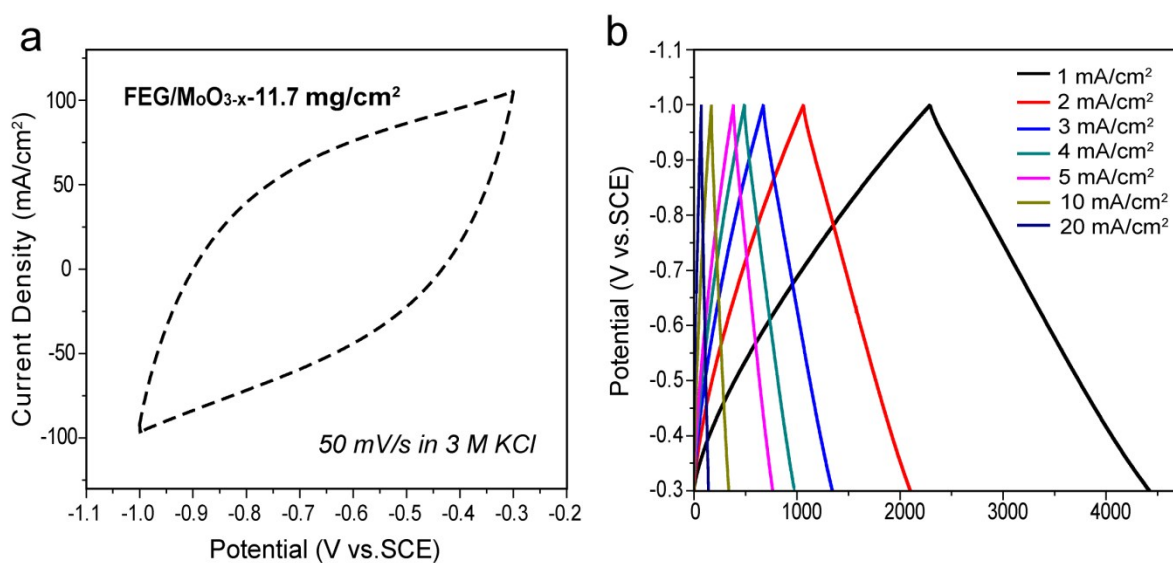


Fig. S16 (a) CV curve of FEG/MoO_{3-x} (11.7 mg cm⁻²) electrode measured at a scan rate of 50 mV s⁻¹.

(b) GCD profiles of FEG/MoO_{3-x} (11.7 mg cm⁻²) collected at various current densities.

Table S1 Summary of capacitive performance of the molybdenum oxide-based electrodes

Sample	Areal capacitance (maximum)	Areal capacitance (minimum)	Rate capability	Mass loading (mg cm ⁻²)
Mo _y O _x (Mo ₈ O ₂₃ and MoO ₃) ^{S2}	1080 mF cm ⁻² at 2 mA cm ⁻²	not report	not report	1
MoO ₃ @PPy ^{S3}	2800 mF cm ⁻² at 4 mA cm ⁻²	800 mF cm ⁻² at 15 mA cm ⁻²	28.6% (4-15 mA cm ⁻²)	2
α-MnO ₂ /h-MoO ₃ ^{S4}	132 mF cm ⁻² at 0.32 mA cm ⁻²	not report	not report	0.32
Sandwich MoO ₃ ^{S5}	496.5 mF cm ⁻² at 1.5 mA cm ⁻²	351 mF cm ⁻² at 15 mA cm ⁻²	70.6% (1.5-15 mA cm ⁻²)	1.5
α-MoO ₃ /grapheme ^{S6}	3600 mF cm ⁻² at 2 mA cm ⁻²	not report	not report	10
MoO ₃ ^{S7}	392.4 mF cm ⁻² at 0.9 mA cm ⁻²	288 mF cm ⁻² at 9 mA cm ⁻²	73% (0.9-9 mA cm ⁻²)	1.8
VO _x @MoO ₃ ^{S8}	1980 mF cm ⁻² at 2 mA cm ⁻²	not report	not report	3.1
graphene@NiO/MoO ₃ ^{S9}	2144 mF cm ⁻² 6 mA cm ⁻²	1372 mF cm ⁻² at 42 mA cm ⁻²	64% (6-42 mA cm ⁻²)	0.85
MoO ₃ @Carbon Cloth ^{S10}	757.9 mF cm ⁻² at 2.2 mA cm ⁻²	634.7 mF cm ⁻² at 22 mA cm ⁻²	29.8% (2.2-22 mA cm ⁻²)	1.1
MoO _{3-x} ultralong nanobelts ^{S11}	990 mF cm ⁻² at 1.8 mA cm ⁻²	634.7 mF cm ⁻² at 36 mA cm ⁻²	51% (1.8-36 mA cm ⁻²)	1.8
TiO ₂ /RGO/MoO ₂ @Mo ^{S12}	3927 mF cm ⁻² at 3 mA cm ⁻²	2748 mF cm ⁻² at 20 mA cm ⁻²	70% (3-20 mA cm ⁻²)	2.4
MoO ₂ /GC-NT _s ^{S13}	1411 mF cm ⁻² at 2.5 mA cm ⁻²	926 mF cm ⁻² at 25 mA cm ⁻²	65.6% (2.5-25 mA cm ⁻²)	5
FEG/MoO_{3-x}	4340 mF cm⁻² at 1 mA cm⁻²	3885 mF cm⁻² at 5 mA cm⁻²	80% (1-10 mA cm⁻²)	15.4
	4145 mF cm⁻² at 2 mA cm⁻²	3471 mF cm⁻² at 10 mA cm⁻²	67% (1-20 mA cm⁻²)	
	4032 mF cm⁻² at 3 mA cm⁻²			
	3948 mF cm⁻² at 4 mA cm⁻²	2940 mF cm⁻² at 20 mA cm⁻²		

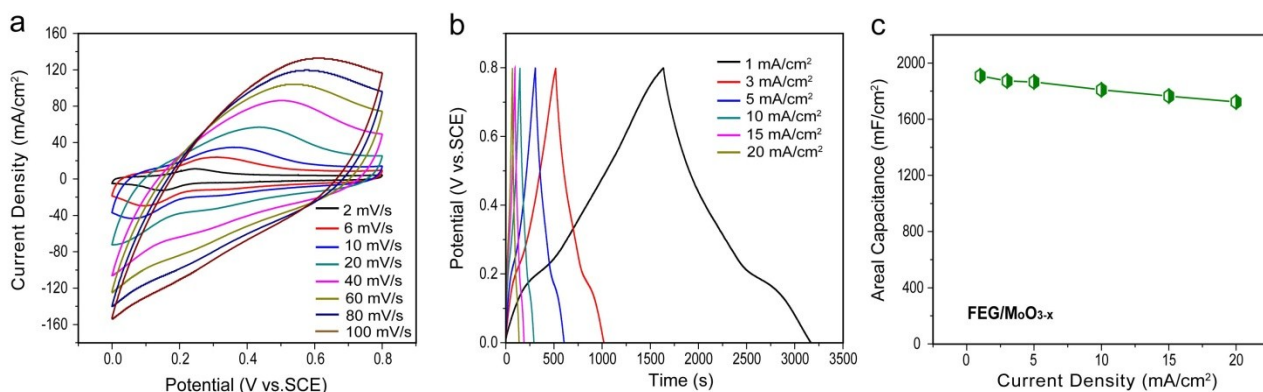


Fig. S17 (a) CV curves of the FEG/MoO_{3-x} electrode measured at different scan rates in 0.5 M H₂SO₄ electrolyte. (b) GCD profiles and (c) areal capacitance of FEG/MoO_{3-x} collected at various current densities.

Dunn Method Analysis

The Dunn method is frequently used to separate the contributions of the capacitive elements of the charge storage and diffusion-controlled insertion processes. The main steps involved in the analysis are as follows:

The scan rate (ν)-dependent current (i) is described by the generic reaction:

$$i = a\nu^b \quad (\text{Equation S10})$$

where a is a constant that depends on the electrode area, the concentration of redox centers, and the diffusion coefficient for the charge transport in the electrode. Two limiting values exist for b : $b = 0.5$ for a voltammetric process that is controlled by linear diffusion to a planar electrode surface while $b = 1.0$ for surface-limited processes including double-layer charging and pseudocapacitive fast charge transfer at surface centers.

By examining the scan rate dependence of the current, one can estimate that the current at each

potential is the sum of both contributions to the capacitance using the following equation:

$$i(v) = k_1 v + k_2 v^{1/2} \quad (\text{Equation S11})$$

where $i(v)$ is the current at a given potential, k_1 and k_2 are constants, and v is the scan rate. In this equation, $k_1 v$ represents the capacitive elements or elements where di/dv is constant while $k_2 v^{1/2}$ represents the diffusion controlled bulk reactions where $di/dv^{1/2}$ is constant. If we divide both sides of this equation with the square root of the scan rate, then we get the following equation:

$$i(v)/v^{1/2} = k_1 v^{1/2} + k_2 \quad (\text{Equation S12})$$

Therefore, if we plot the $i/v^{1/2}$ at a given potential versus $v^{1/2}$, we should obtain a line with the slope equaling constant k_1 and the y -intercept equaling k_2 , thus giving us a quantitative way of separating the capacitive elements, $k_1 v$, from the bulk reactions, $k_2 v^{1/2}$, at each given voltage.

4. Electrochemical performance of functionalized partial-exfoliated graphite (FEG)

The electrochemical performances of the FEG electrode was conducted in a three electrode cell containing 3 M KCl electrolyte with SCE electrode as the reference electrode and graphite foil as the counter electrode. Fig. S18a shows the CV curves for the FEG collected at different scan rates. As can be seen, no significant distortion was observed from the CV curves with the increase of scan rate, suggesting a good rate capability. Fig. S18b provides the galvanostatic charge-discharge curves recorded at various current densities of 1-20 mA cm⁻². Based on the galvanostatic charge-discharge curves collected at 1 mA cm⁻², the areal capacitance of FEG was determined to be 2.3 F cm⁻². The high capacitance of FEG cathode, as well as those of the FEG/MoO_{3-x} anode, ensure the excellent overall electrochemical performance of the FEG/MoO_{3-x}//FEG ASC.

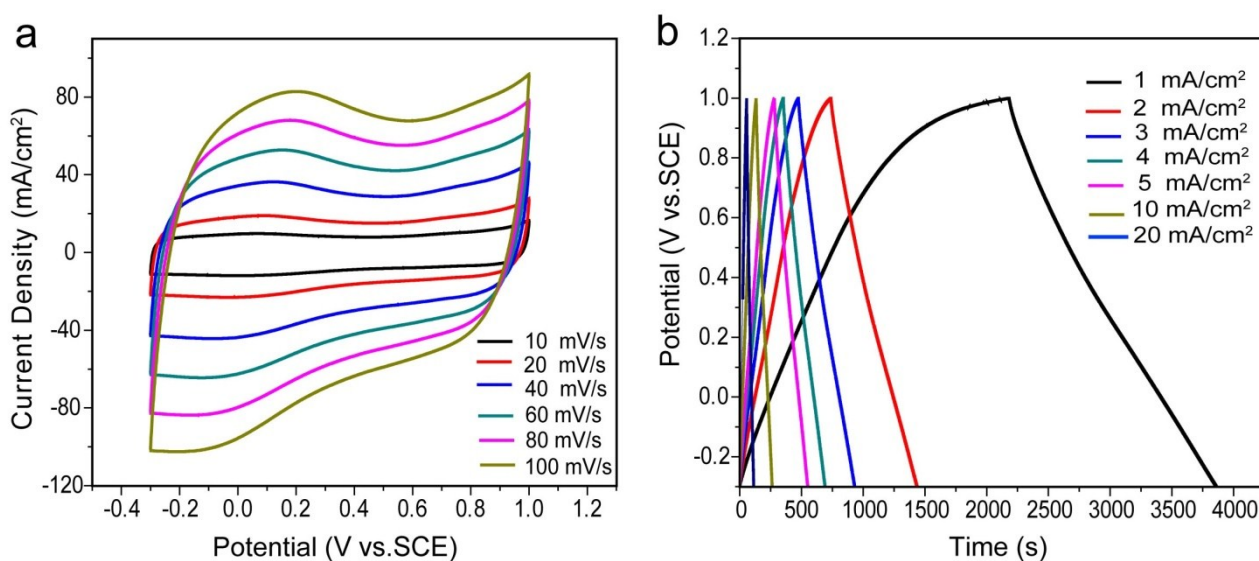


Fig. S18 (a) CV curves of the FEG electrode measured at different scan rates. (b) GCD profiles of FEG collected at various current densities.

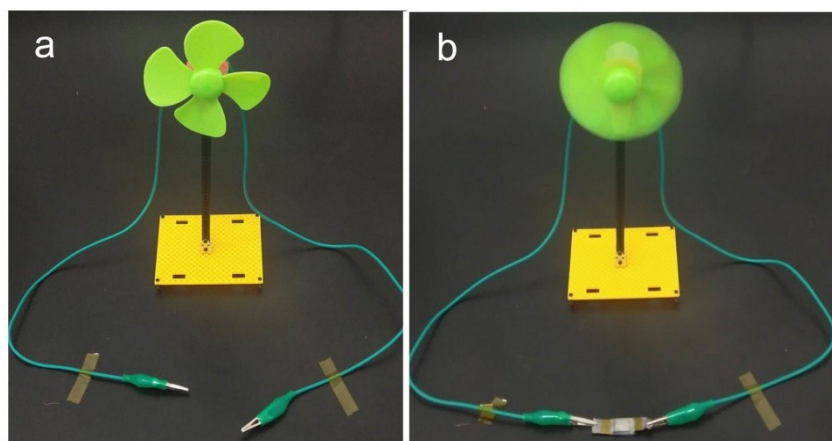


Fig. S19 The optical images of an electrical fan powered by FEG/MoO_{3-x}//FEG device.

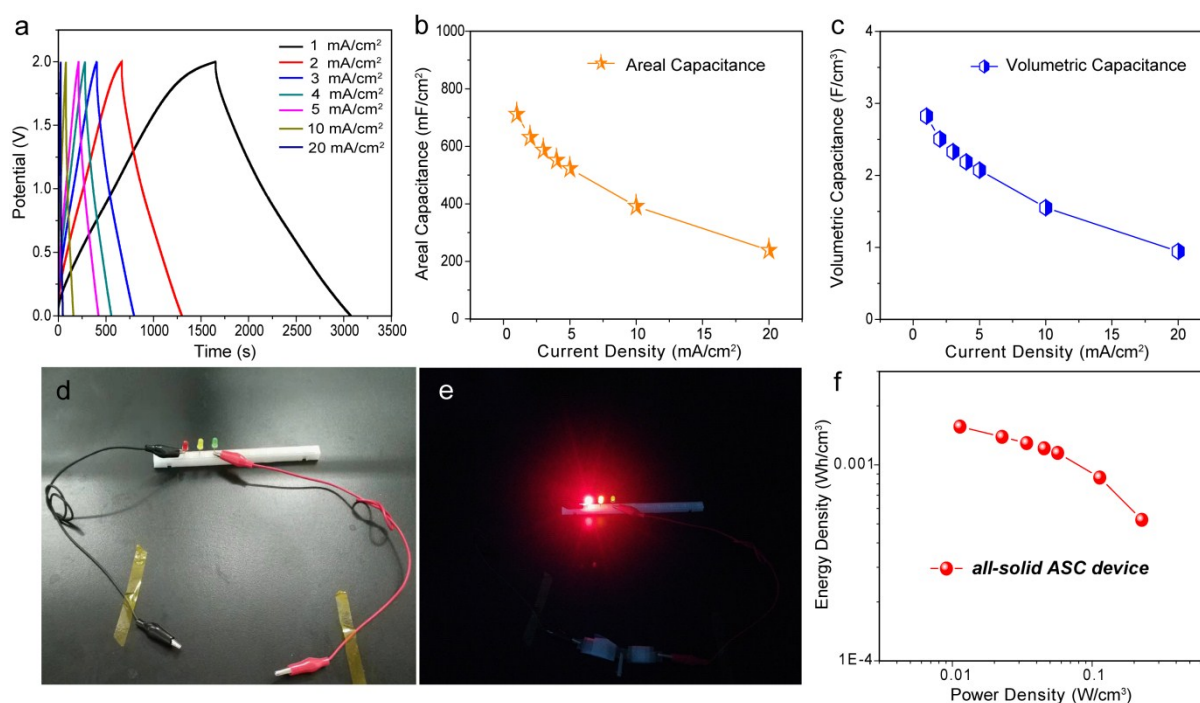


Fig. S20 (a) GCD profiles of the all-solid ASC device collected at various current densities. (b) Areal and (c) volumetric capacitance of the all-solid ASC device measured at different current densities. (d) and (e) The fully charged solitary ASC operates LED lighting matrix. (f) Ragone plot of the all-solid ASC device.

References

- S1 Y. Song, T. Y. Liu, G. L. Xu, D. Y. Feng, B. Yao, T. Y. Kou, X. X. Liu and Y. Li, *J. Mater. Chem. A*, 2016, **4**, 7683-7688.
- S2 N. Maheswari, G. Muralidharan, *Appl. Surf. Sci.*, 2017, **416**, 461-469.
- S3 S. W. Zhang, B. S. Yin, C. Liu, Z. B. Wang and D. M. Gu, *Chem. Eng. J.*, 2017, **312**, 296-305.
- S4 P. M. Shafi, R. Dhanabal, A. Chithambararaj, S. Velmathi and A. C. Bose, *ACS Sustainable Chem. Eng.*, 2017, **5**, 4757-4770.
- S5 H. Ji, X. Liu, Z. Liu, B. Yan, L. Chen, Y. Xie, C. Liu, W. Hou and G. Yang, *Adv. Funct. Mater.*, 2015, **25**, 1886-1894.
- S6 J. Zhou, J. Song, H. Li, X. Feng, Z. Huang, S. Chen, Y. Ma, L. Wang and X. Yan, *New J. Chem.*, 2015, **39**, 8780-8786.
- S7 H. C. Xuan, Y. Q. Zhang, Y. K. Xu, H. Li, P. D. Han, D. H. Wang and Y. W. Du, *Phys. Status Solidi A*, 2016, **213**, 2468-2473.
- S8 S. Q. Wang, X. Cai, Y. Song, X. Sun and X. X. Liu, *Adv. Funct. Mater.*, 2018, **28**, 1803901.
- S9 W. Zeng, G. Zhang, S. Hou, T. Wang and H. Duan, *Electrochim. Acta*, 2015, **151**, 510-516.
- S10 K. Lu, B. Song, K. Li, J. Zhang and H. Ma, *J. Power Sources*, 2017, **370**, 98-105.
- S11 L. Huang, B. Yao, J. Sun, X. Gao, J. Wu, T. Li, Z. Hu and J. Zhou, *J. Mater. Chem. A*, 2017, **5**, 2897-2903.
- S12 P. Ju, Z. Zhu, X. Shao, S. Wang, C. Zhao, X. Qian and C. Zhao, *J. Mater. Chem. A*, 2017, **5**, 18777-18785.
- S13 Y. Zhang, S. Yang, S. Wang, H. K. Liu, L. Li, S. X. Dou and X. Liu, *Small*, 2018, **14**, 1800480.